LAWRENCE
LIVERMORE
NATIONAL
LABORATORY

LLNL-PROC-557665

Precision Magnet Measurements for X-Band Accelerator Quadrupole Triplets

R. A. Marsh, S. G. Anderson, J. P. Armstrong

May 17, 2012

IPAC 2012
New Orleans, LA, United States
May 20, 2012 through May 25, 2012

Disclaimer

PRECISION MAGNET MEASUREMENTS FOR X-BAND ACCELERATOR QUADRUPOLE TRIPLETS *

R.A. Marsh†, S.G. Anderson, J.P. Armstrong
Lawrence Livermore National Laboratory, Livermore, CA 94550, USA

Abstract

An X-band test station is being developed at LLNL to investigate accelerator optimization for future upgrades to mono-energetic gamma-ray (MEGa-Ray) technology at LLNL. Beamline magnets will include an emittance compensation solenoid, windowpane steering dipoles, and quadrupole magnets. Demanding tolerances have been placed on the alignment of these magnets, which directly affects the electron bunch beam quality. A magnet mapping system has been established at LLNL in order to ensure the delivered magnets match their field specification, and the mountings are aligned and capable of reaching the specified alignment tolerances. The magnet measurement system will be described which uses a 3-axis Lakeshore gauss probe mounted on a 3-axis translation stage. Alignment accuracy and precision will be discussed, as well as centering measurements and analysis. The dependence on data analysis over direct multi-pole measurement allows a significant improvement in useful alignment information. Detailed analysis of measurements on the beamline quadrupoles will be discussed, including multi-pole content both from alignment of the magnets, and the intrinsic level of multi-pole magnetic field.

INTRODUCTION

As part of ongoing Mono-Energetic Gamma-ray (MEGa-ray) efforts at LLNL, a 250 MeV X-band accelerator has been designed (VELOCIRAPTOR) [1]. The photoinjector for this machine will be a 5.59 cell rf gun jointly developed by LLNL and SLAC [2]. This Mark 1 rf gun will first be tested at LLNL on an X-band test station that is currently under fabrication [3]. Most components for this test station have been fabricated and are currently being installed in B194 at LLNL. The X-band photoinjector has been designed to generate 250 pC bunches at 0.35 mm mrad normalized rms emittance. To preserve this emittance, tolerances have been established on the alignment of many test station and linac components, including the emittance compensation solenoid and rf quadrupole focussing triplets. A magnet test stand has been developed to quickly and accurately align the mechanical and magnetic centers on the rf quadrupole magnets manufactored by *RadiaBeam Technologies*, as well as provide testing capability for other linac magnets.

* This work performed under the auspices of the U.S. Department of Energy by Lawrence Livermore National Laboratory under Contract DE-AC52-07NA27344

† marsh19@llnl.gov

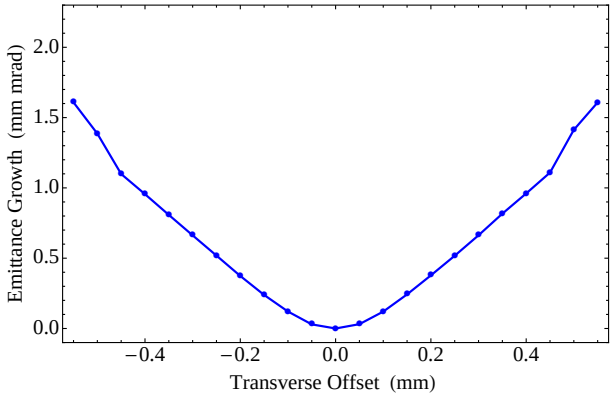

Figure 1: Magnet misalignment effect on *PARMELA* simulated emittance growth.

MAGNET TEST SETUP

The magnet test setup is shown in Fig. 2 and is comprised of: a *Velmex* 3-axis translation stage, a *Lakeshore* 3-axis Gauss probe, and a PC for control and data acquisition. Two quadrupole triplets can be seen on adjustable mounts, as well as the photoinjector emittance compensation solenoid on the floor in the background. The translation stage is specified to $\sim$ 5 μm accuracy, precision, and reproducibility, with sufficient travel to probe each quadrupole triplet. The Lakeshore probe contains 3 orthogonal flux surfaces, and measures the x, y, and z components of the magnetic field (B_x, B_y, and B_z) at slightly different positions (which is corrected for in data analysis). The probe, stage, and magnet are aligned with the optical table. The probe is fiducialized with respect to the magnet by optical inspection of the probe position with respect to the front magnet pole faces. This alignment method achieves $\sim$ 50 μm precision, which is sufficient for these measurements.

The *LabView* data acquisition program has been written to control the magnet power supplies, move the stage, make the field measurement, and store the resulting data. The GUI for the program is visible on the left side of the monitor in Fig. 2. Debugging and improvements in user operability were implemented during magnet measurement taking, as well as optimization of motor speed, field measurement dwell time, and step resolution. Saturation in each magnet was measured, as well as the transverse field at a fixed current, before detailed 3D scans were taken of each complete triplet. The first 3D scan revealed single step ($\sim$ 5μm) whiplash as a result of $\sim$ 20 successive raster

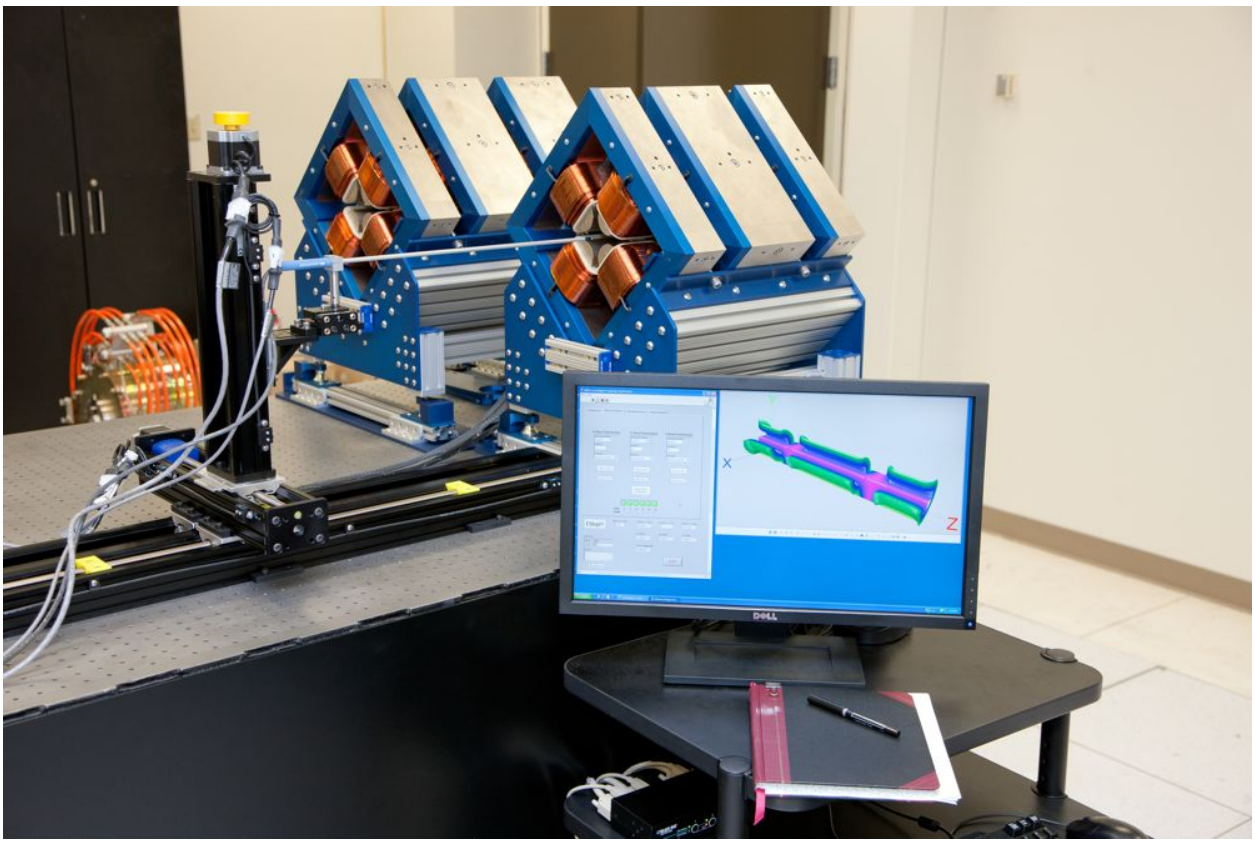

Figure 2: Magnet measurement arrangement: quadupole magnets, Gauss probe on translation stage and control interface with field visualization.

scan in one direction (x) for each scan across the other (y). In order to minimize this effect, boustrophedon scanning was implemented in which data is taken in both the $+x$ and $-x$ directions at successive y points. Data for further analysis was taken on a 1 mm size grid extending within 2 mm of the pole pieces, resulting in measurement of B_x, B_y, and B_z at nearly 200,000 points.

MAGNET FIELD ANALYSIS

Field visualization was accomplished by extracting line-plot of pertinent data, or in the bulk using the volume visualization tool *Slicer Dicer*. A typical plot is visible on the right side of the monitor in Fig. 2. The magnetic center is determined in a quadrupole field by the zero-crossing of the field component with respect to the orthogonal dimension; that is, the x zero is determined by the field crossing of B_y, and similarly the y zero is determined by the field crossing of B_x. The process is repeated for each z slice of field data, in order to determine the magnetic center as a function of longitudinal displacement along the beam axis. The x magnetic center data is shown in Fig. 3 for one of the quadrupole triplets: the gridlines indicate the flat field profile regions, with large excursions in the calculated center resulting from small magnetic field values near the zero crossing between individual quadrupole magnets in the triplet.

The probe was rotated $45°$ and data was reacquired using the same magnet, allowing precise determination of the internal position of the magnetic flux surfaces within the probe: 2.20 mm in x and -2.10 mm in y. The magnetic center to physical center alignment for both of the mounted triplets was within 100 μm which is the specified tolerance, so that no magnet-by-magnet shimming was necessary.

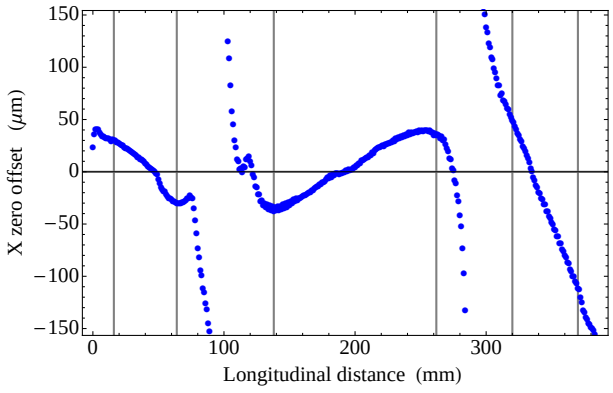

Figure 3: Quadrupole magnet field slice analysis showing magnetic center as a function of longitudinal position.

The multipole content of each quadrupole magnet gives

a direct measurement on field errors, as well as alignment of the the physical or measuring axis to the magnetic axis. The vector magnetic field as a function of position, $B(z)$ at a given position, $z = x + \imath y$, can be written as:

$$\begin{aligned} B(z) &= B_y(x,y) + \imath B_x(x,y) \\ &= \sum_{n=1}^{\infty} (B_n + \imath A_n)(z)^{n-1} \end{aligned} \tag{1}$$

where $B_x(x,y)$ and $B_y(x,y)$ are the x and y components of the magnetic field respectively [4]. For an ideal quadrupole magnet, an offset in measuring axis with respect to the magnetic axis manifests as a dipole term. For non-ideal quadrupole magnets, additional higher order terms are expected as well. The field data from magnet measurement using this technique provides a very large number of points for curve fitting, allowing slice-by-slice decomposition into dipole, quadrupole, sextupole, octupole, and higher order multipole components. The decomposition of field into components is shown in Fig. 4 for each transverse scan as a function of longitudinal (z) distance. A clear hierarchy of terms is visible on the logarithmic scale. The gridlines indicate the flat field profile regions, showing divergence where expected as the fields cross zero between quadrupole magnets.

Improvements in fiducialization could make the system more accurate down to 5 μm which is the limit of the current stage.

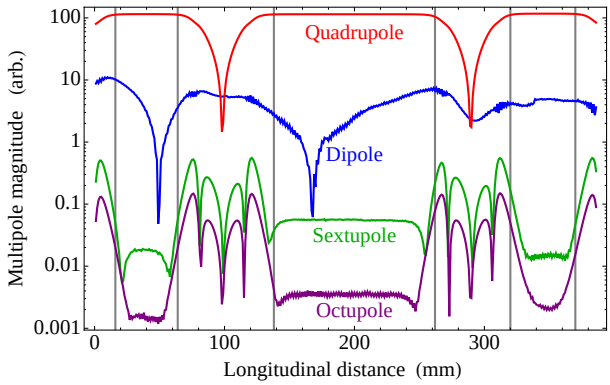

Figure 4: Quadrupole magnet field slice decomposition into multipole components: dipole term in red, quadrupole in blue, sextupole in green, octupole in purple.

REFERENCES

[1] S.G. Anderson, *et al.*, Nucl. Instrum. Methods Phys. Res., Sect. A, **657** 1, pages 140–149 (2011).

[2] R.A. Marsh, *et al.*, Phys. Rev. ST Accel. Beams, *submitted* (2012).

[3] R.A. Marsh, *et al.*, *"X-band Test Station at LLNL"* **MOPC067**, *IPAC 2011*.

[4] "Handbook of Accelerator Physics and Engineering", edited by A.W. Chao and M. Tigner, World Scientific, Singapore, 2006.